A Novel Type of Isomerism in [3]Catenanes**

Peter R. Ashton, Sue E. Boyd, Christian G. Claessens, Richard E. Gillard, Stephan Menzer, J. Fraser Stoddart,* Malcom S. Tolley, Andrew J. P. White, and David J. Williams

Abstract: The self-assembly of three [3]-catenanes based on a single tetracationic cyclophane—cyclobis(bipyridinium-1,4-diethoxybenzene)—with pairs of identical interlocked crown ethers—bis-*p*-phenylene[34]crown-10, bis-1,5-dioxynaphthalene[38]crown-10, or tetrafluoro-*p*-phenylene-*p*-phenylene[34]crown-10—has been achieved in yields of 34, 31, and 33%, respectively. The solid-state structures of these [3]catenanes, determined by X-ray crystallography, are consistent with molecules having approximately C_{2h} symmetry. In the solution state, the π-electron rich aromatic ring systems of the crown ether components, residing within the cavity of the tetracationic cyclophane, can adopt two different relative orientations, thus giving rise to two distinct isomeric forms possessing either C_{2h} or D_2 symmetries. Two dynamic processes have been characterized in the [3]catenane incorporating bis-1,5-dioxynaphthalene[38]-crown-10 macrocycles, by means of variable-temperature ^{1}H NMR spectroscopy and subsequent lineshape analyses. The slower process is the exchange between C_{2h} and D_2 isomers, and the faster process is the rotation of the bipyridinium units of the cyclophane around their N···N axes. The evaluation of the free energies of activation at 298 K, which are, for the slower process, ca. 16 kcal mol^{-1}, and for the faster one, ca. 14.5 kcal mol^{-1}, has enabled us to propose a scenario in which the two included 1,5-dioxynaphthalene ring systems move continuously about the center of the cavity of the tetracationic cyclophane. A partial dissociation of one 1,5-dioxynaphthalene ring system allows the adjacent bipyridinium units to rotate about their long axes, whereas a complete dissociation is presumably necessary to allow a 1,5-dioxynaphthalene ring system to rotate about its O···O axis. The isomerism between the C_{2h} and the D_2 isomers of the [3]catenane incorporating the two bis-1,5-dioxynaphthalene[38]crown-10 rings is dependent upon 1) translational motions between the two crown ether rings and the central tetracationic cyclophane and 2) conformational changes within at least one of the two crown ether rings.

Keywords
catenanes · dynamics · isomerization · NMR spectroscopy · self-assembly

Introduction

Nature is expert at employing self-assembly processes[1] for the construction of complex molecular assemblies and supramolecular arrays. The exceptional features and properties of this synthetic paradigm have aroused the attention of chemists in recent years, to the extent that an increasing number of examples of fully synthetic self-assembling systems have been reported[1-14] in the literature since around the mid-1980s. Catenanes,[2] that is, compounds composed of molecules made up of interlocked rings, were first synthesized by using statistical,[3] Möbius strip,[4] or directed-synthesis approaches.[5] It is now clear, however, that catenanes can be obtained far more efficiently by using either templating methodologies[6] relying upon, for example, metal–ligand interactions,[7, 8] hydrogen bonds,[9] and/or π–π interactions.[10-13] Numerous examples of the template-directed synthesis of [2]catenanes have appeared in the literature over the past decades,[7, 9, 10] but only a few higher catenanes have been fully described.[8, 11-14] The self-assembled [3]catenanes, **1**·4PF$_6$ and **2**·4PF$_6$, are composed (Figure 1) of two identical crown ether molecules, interlocked with one large tetracationic cyclophane, containing two bipyridinium units and two bitolyl units. It transpires that the following interactions provide the driving force for the self-assembly of these interlocked molecules:

1) π–π interactions[15] between π electron rich and deficient aromatic rings.
2) [C–H···O] hydrogen bonding interactions[16] between acidic hydrogen atoms in the α-position of the bipyridinium

[*] Prof. J. F. Stoddart, Dr. S. E. Boyd, Dr. C. G. Claessens,[+] R. E. Gillard, P. R. Ashton, M. S. Tolley
School of Chemistry, University of Birmingham
Edgbaston, Birmingham B15 2TT (UK)
Fax: Int. code +(121)414-3531
Prof. D. J. Williams, Dr. S. Menzer, Dr. A. J. P. White
Department of Chemistry, Imperial College
South Kensington, London SW7 2AY (UK)
Fax: Int. code +(171)594-5804
[+] Permanent address: Ecole Normale Supérieure de Lyon
Stéréochimie et Interactions Moléculaires
46, Allée d'Italie, 69364 Lyon cedex 07 (France)
Fax: Int. code +(4)7272-8483

[**] Molecular Meccano, Part 20; for Part 19, see: M. Asakawa, P. R. Ashton, W. Dehaen, G. L'abbé, S. Menzer, J. Nouwen, F. M. Raymo, J. F. Stoddart, M. S. Tolley, S. Toppet, A. J. P. White, D. J. Williams, *Chem. Eur. J.* **1997**, *3*, 772.

0947-6539/97/0305-0788 $ 17.50+.50/0

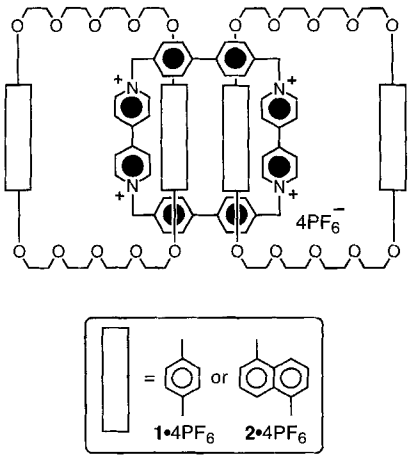

Figure 1. The [3]catenanes **1**·4PF$_6$ and **2**·4PF$_6$.

units in the tetracationic cyclophane and some of the polyether oxygen atoms in the crown ethers.

3) Edge-to-face T-type interactions[17] between hydrogen atoms attached to the π electron rich aromatic rings of the crown ethers and the π systems associated with the aromatic spacers separating the bipyridinium units in the tetracationic cyclophane.

This built-in information "lives on" within their molecular structures, giving rise to their fascinating chemical and physical properties. We believe that a better understanding of the dynamic aspects of the structures of these molecular compounds would help us to conceive and realize new molecular assemblies and supramolecular arrays, which could ultimately prove valuable in the development of new materials and/or functioning molecular devices.

Here, we report on the self-assembly (Scheme 1) of the three new [3]catenanes **6a**·4PF$_6$, **6b**·4PF$_6$, and **6c**·4PF$_6$, analogues of **1**·4PF$_6$ and **2**·4PF$_6$ in which the spacer units in the central tetracationic cyclophanes have been modified to incorporate extended hydroquinone-containing units. The structures of these compounds have been fully characterized by ^{1}H NMR spectroscopy in solution and by X-ray crystallography in the solid state. From the ^{1}H NMR spectroscopic data, we have been able to examine the dynamic behavior of the [3]catenanes in considerable detail. In particular, careful lineshape analyses[18] of the 400 MHz ^{1}H NMR spectra of **6a**·4PF$_6$, recorded at different temperatures, have enabled us to identify, in quantitative terms, the precise nature of the dynamic processes taking place between the three interlocked rings in this [3]catenane.

Results and Discussion

Synthesis: The dibromide **3** was treated[19] with 4,4′-bipyridine in refluxing MeCN to yield bipyridine salt **4**·2PF$_6$ after counterion exchange (NH_4PF_6/H_2O). The catenations were carried out by reaction of **3** and **4**·2PF$_6$ in DMF under high-pressure conditions (12 kbar, 20 °C) with the crown ethers **5a**,[20a] **5b**,[10b] and **5c**,[20b] affording (Scheme 1), after counterion exchange, the [3]catenanes **6a**·4PF$_6$, **6b**·4PF$_6$, and **6c**·4PF$_6$ in yields of 34, 31, and 33%, respectively. The same reactions, carried out at ambient pressure and room temperature with

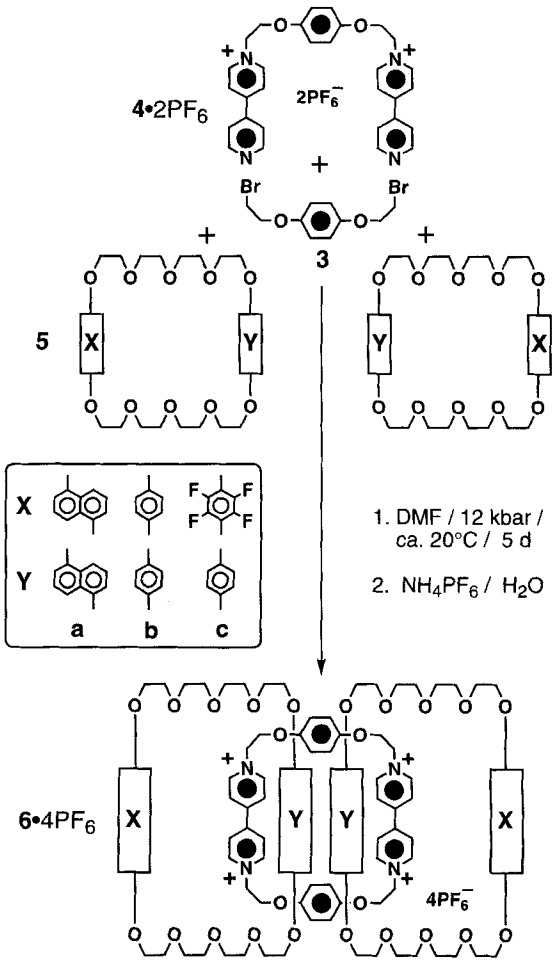

Scheme 1. The template-directed syntheses of the [3]catenanes **6a**·4PF$_6$, **6b**·4PF$_6$ and **6c**·4PF$_6$.

crown ethers **5a** and **5b** in MeCN, yielded only 1.1% of **6a**·4PF$_6$ and 0.8% of **6b**·4PF$_6$ even after a 9-week period. No [3]catenanes were detected in reaction mixtures in which MeCN had been replaced by DMF as the solvent. These results underline the almost complete lack of reactivity of the dibromide **3** at room pressure when compared with the high reactivities of the benzylic dibromides, commonly used in the self-assembly of related catenanes.[10–13]

Mass Spectrometry: The [3]catenanes **6a**·4PF$_6$, **6b**·4PF$_6$, and **6c**·4PF$_6$ were characterized by obtaining their LSI mass spectra, which revealed peaks corresponding to the successive loss of PF_6^- counterions from their molecular ions. In all cases, we observed the $[M - PF_6]^+$, $[M - 2PF_6]^+$, and $[M - 3PF_6]^+$ ions (Table 1). In addition, peaks attributable to the loss of one, two,

Table 1. LSIMS [a] data for the [3]catenanes **6a**·4PF$_6$, **6b**·4PF$_6$, and **6c**·4PF$_6$.

Compound	M	$M - PF_6$	$M - 2PF_6$	$M - 3PF_6$
6a·4PF$_6$	(2492) [b]	2347	2202	2057
6b·4PF$_6$	(2292) [b]	2147	2002	1857
6c·4PF$_6$	2436	2291	2146	2001

[a] LSIMS were recorded on a VG ZabSpec mass spectrometer, using a *m*-nitrobenzyl alcohol matrix and a scan speed of 10 s per decade. [b] The numbers in parentheses refer to peaks that were not observed.

three, and four PF_6^- counterions from the corresponding [2]catenanes, formed as the result of the cleavage of one of the macrocyclic polyether rings in the [3]catenanes, were observed. The LSI mass spectrum of **6a**·4PF$_6$ is reproduced in Figure 2.

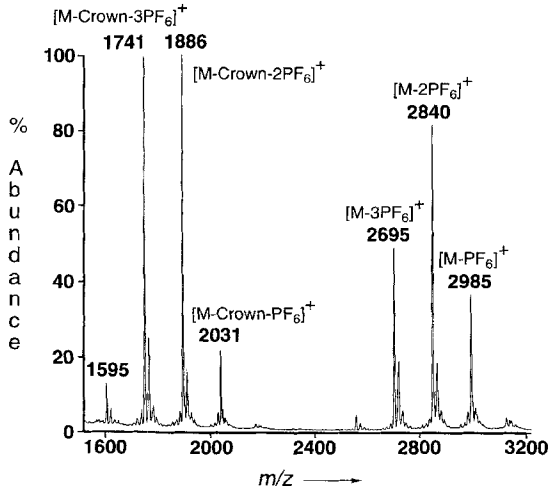

Figure 2. The LSI MS of the [3]catenane **6a**·4PF$_6$.

X-Ray Crystallography: The X-ray crystal structural analysis (Figures 3 and 4, Table 2) of **6a**·4PF$_6$ demonstrates that the mode of threading of the pairs of 1,5-DNP38C10 (**5a**) macrocycles through the center of the tetracationic cyclophane is to all intents and purposes unchanged in comparison with the situation that pertains in the [3]catenanes containing the cyclobis(paraquat-4,4′-biphenylene) tetracation.[12] The principal difference is in the nature of the noncovalent interactions between the components. The familiar pattern of DADDAD π-stacking between the donor (D) 1,5-DNP38C10 ring systems and the acceptor (A) bipyridinium units is present. Similarly, there are

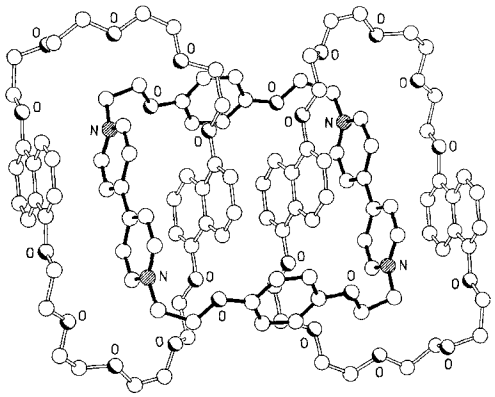

Figure 3. Ball-and-stick representation of the solid-state structure of the [3]catenane **6a**·4PF$_6$.

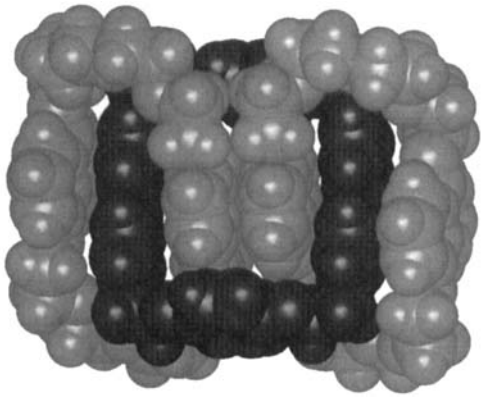

Figure 4. Space-filling representation of the solid-state structure of the [3]catenane **6a**·4PF$_6$.

supplementary [C–H···O] hydrogen bonding interactions[16] between two diametrically opposite CH_2N^+ hydrogen atoms in the tetracationic cyclophane component and oxygen atoms of the 1,5-DNP38C10 component. However, conventional edge-

Table 2. Distances [a] (Å) and angles [a] (°) characterizing the molecular and supramolecular geometries of the [3]catenanes **6a**·4PF$_6$, **6b**·4PF$_6$, and **6c**·4PF$_6$.

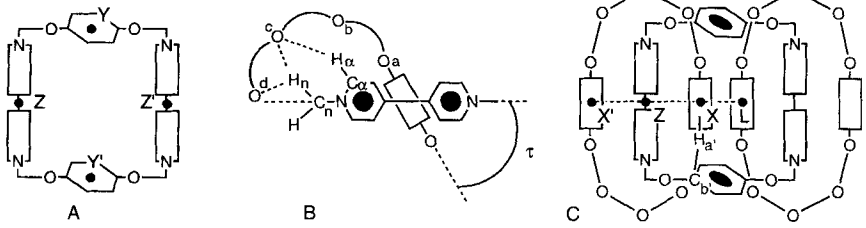

Compound	Z···Z′ (Å)	Y···Y′ (Å)	θ [c] (°)	τ "inside" (°)	τ "outside" (°)	X′···Z (Å)	Z···X (Å)	X···L (Å)	[H_n···O_c] (Å) [C_n···O_c] (Å) [C_n–H_n···O_c] (°)	[H_n···O_d] (Å) [C_n···O_d] (Å) [C_n–H_n···O_d] (°)	[$H_{a'}$···$C_{b'}$] (Å) [X–$H_{a'}$···$C_{b'}$] (°)
6a·4PF$_6$	10.4	10.9	13	47	9	3.43	3.36	3.52	– – –	2.47 3.40 162	2.85 134
6b·4PF$_6$ [b]	10.8	10.1	23	41	18	3.47	3.42	3.50	2.32 3.12 141	– – –	2.68 171
6c·4PF$_6$	10.5	10.1	27	35	13	3.59	3.38	3.55	2.45 3.28 145	– – –	2.70 165

[a] The distances and angles indicated in the table are illustrated in the diagrams A, B, and C shown above. [b] In **6**·4PF$_6$ there is a supplementary hydrogen bond between H_z and O_c whose characteristic parameters are: [H_z···O_c] = 2.30 Å, [C_z···O_c] = 3.12 Å, [C_z–H_z···O_c] = 141°. [c] θ is the angle of tilt of the hydroquinone rings with respect to the perpendiculars of the mean planes of the cyclophanes.

0947-6539/97/0305-0790 $ 17.50+.50/0 Chem. Eur. J. 1997, 3, No. 5

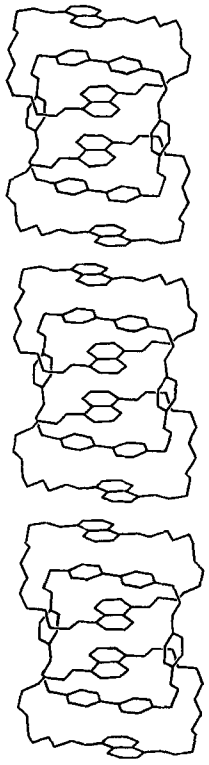

Figure 5. Part of the continuous DADDAD stack associated with the [3]catenane **6a**·4PF$_6$.

to-face interactions, involving the "inside" naphthalene rings and the extended hydroquinone spacer units within the cyclophane, are not possible because of the presence of only a single, centrally positioned, aromatic ring. Despite this modification, one of the *peri* naphthalene hydrogen atoms is directed toward one of the *para*-substituted carbon atoms of the hydroquinone ring in the cyclophane. The [H···C] distance of 2.85 Å is compatible with a [CH···π] interaction,[17] consistent with the π system extending beyond the periphery of the hydroquinone ring.

The pattern of intracatenane π–π stacking extends (Figure 5) to include symmetry-related molecules in the crystal, the stacking involving the "alongside"-positioned 1,5-dioxynaphthalene ring system. The hydroquinone rings of the cyclophane are not involved in any intermolecular π–π interactions. It is interesting to note that the inter- and intracatenane stacking geometries of the 1,5-dioxynaphthalene ring systems, though differing in their relative degrees of overlap, both retain the "eclipsed" relationship for the two matching ring systems, the internal one being a consequence of the crystallographically-imposed C_i symmetry of the [3]catenane. This geometry contrasts with the situation in solution where two isomers approaching C_{2h} and D_2 symmetries are present, that is, in the solid state only one of the isomers, namely isomer **B** (see below), possessing a near C_{2h} symmetry, is present.

The solid-state structure (Figure 6) of the [3]catenane **6b**·4PF$_6$ in which the 1,5-DNP38C10 macrocyclic components have been replaced by BPP34C10 (**5b**) is very similar to that of **6a**·4PF$_6$. Although there is the same DADDAD π–π stacking motif present within the [3]catenane, it is interesting to note that in **6b**·4PF$_6$ the "inside" hydroquinone rings both have *anti* geometries for their substituent O–CH$_2$ bonds, while the "alongside" rings have *syn* geometries—a pattern that is the reverse of that observed in the crystalline state of **1**·4PF$_6$.[12] Secondary stabilization of the [3]catenane is achieved by [CH···O] hydrogen bonding involving both α-bipyridinium and CH$_2$N$^+$ hydrogen atoms in the cyclophane and polyether oxygen atoms in the BPP34C10 components (Table 2). As in **6a**·4PF$_6$, we see that one of the "inside" hydroquinone hydrogen atoms is oriented toward the *para*-substituted carbon atoms of the hydroquinone rings within the cyclophane. Inspection of the packing of the [3]catenanes reveals the formation of a "close-packed" sheet array of molecules, but a marked absence of any extended intermolecular π–π stacking interactions.

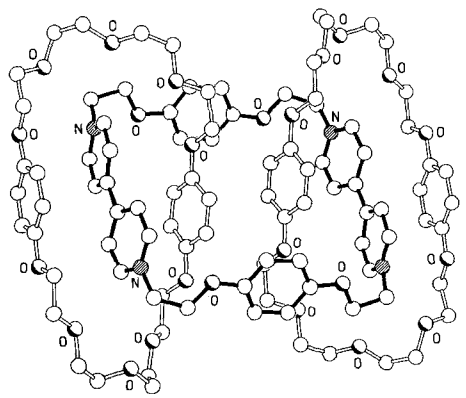

Figure 6. Ball-and-stick representation of the solid-state structure of the [3]catenane **6b**·4PF$_6$.

The X-ray structure (Figure 7) of **6c**·4PF$_6$, in which one of the hydroquinone rings of each BPP34C10 is tetrafluoro-substituted, shows the unsubstituted hydroquinone rings to be positioned, with an *anti*-OCH$_2$ geometry, "inside" the tetracationic cyclophane, the tetrafluoro-substituted rings both being positioned on the "outside". The overall molecular structure is little different from that observed for the [3]catenane **6b**·4PF$_6$, apart from the marked absence of coplanarity of the *para*-substituted OCH$_2$ groups attached to the tetrafluorohydroquinone rings, a local geometry which we have observed previously.[20e] Details of π–π stacking separations and intercomponent hydrogen bonding interactions are given in Table 2. The molecules pack to form an irregular folded sheet array, there being an absence of any inter-[3]catenane π–π stacking interactions.

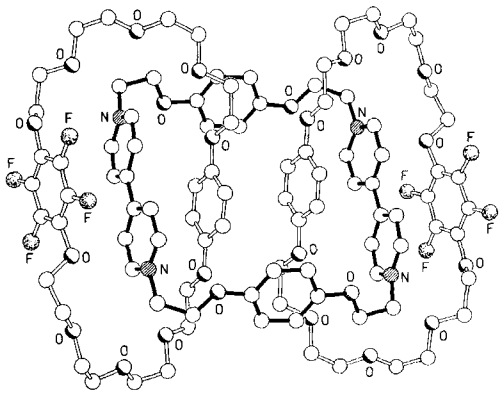

Figure 7. Ball-and-stick representation of the solid-state structure of the [3]catenane **6c**·4PF$_6$.

^{1}H NMR Spectroscopy: The solution-state structure and dynamic behavior of the [3]catenane **6a**·4PF$_6$ were studied using variable-temperature ^{1}H NMR spectroscopy. The spectra revealed the presence in solution of two interconverting isomeric forms of the [3]catenane. In fact, these two isomers are the two possible low-energy (i.e., long lifetime) ground states for the highly fluxional molecule. These "isomers" are distinguished by the local symmetry of the ADDA stack as defined by the relative orientation of the 1,5-dioxynaphthalene residues included within the cavity of the tetracation. At 314 K, the 400 MHz ^{1}H NMR spectrum of a solution of the [3]catenane **6a**·4PF$_6$ in CD$_3$COCD$_3$/CD$_3$NO$_2$ (4:1 *v*/*v*) appears uniformly broad and uninformative. The spectra begin to sharpen and resolve with decreasing temperature until, at temperatures below 260 K, two sets of resonances characterizing the unequally populated iso-

mers **A** and **B** become distinguishable. A further decrease in temperature causes the resonances to sharpen initially and the populations of the isomers **A** and **B** to converge until, at temperatures around 220 K, their ratio approaches 1:1.

The ^{1}H NMR spectrum of **6a**·4PF$_6$ recorded in CD_3COCD_3/CD_3NO_2 (4:1, *v*/*v*) at 238 K is reproduced in Figure 8. Assignments made on the basis of 2D dqf-COSY and NOESY spectra are listed in Table 3. Relevant sections of a 2D NOESY/EXSY experiment, conducted at 238 K, are provided in Figures 9 and 10. The respective local symmetry environments of **A** and **B** are evidenced by the resonances attributable to the hydroquinone ring of the tetracationic cyclophane component of the [3]catenane. Figure 9 shows slices through the transformed NOESY data matrix, isolating the two distinct hydroquinone ring spin systems. Inspection of the multiplets observed for the two AA′ and XX′ spin systems shows two discrete substitution patterns for **A** and **B** in which the two AA′ and XX′ pairs are related by σ and C_2 symmetry operations, respectively. The apparent "broadened doublets" observed (Figure 9a) for **A** are consistent with a disposition of the AA′XX′ nuclei such that the major contributor to the second-order spin system is a relatively large J_{ortho} coupling. By contrast, the second isomer **B** shows only apparent "broadened singlets" (Figure 9b), consistent with a *meta* disposition of the AA′ and XX′ pairs. These results are consistent with **A** possessing D_2 and **B** C_{2h} symmetry. The structural information, relating to the relative positions of the naphthalene ring systems with respect to the bipyridinium units is summarized schematically in Figure 9.

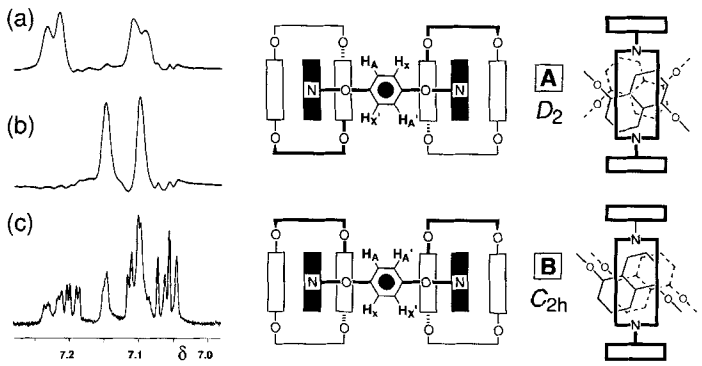

Figure 9. a)/b) Slices taken from the NOESY/EXSY spectrum of **6a**·4PF$_6$ (500 MHz, τ_{mix} = 400 ms, T = 238 K, CD_3COCD_3/CD_3NO_2 (4:1, *v*/*v*)). Resonances attributable to the protons attached to the hydroquinone rings of the tetracation in **A** and **B**, respectively, are highlighted. c) The expansion of the equivalent region of the 1D spectrum (500 MHz, 238 K). Cavity geometries of **A** and **B** are shown.

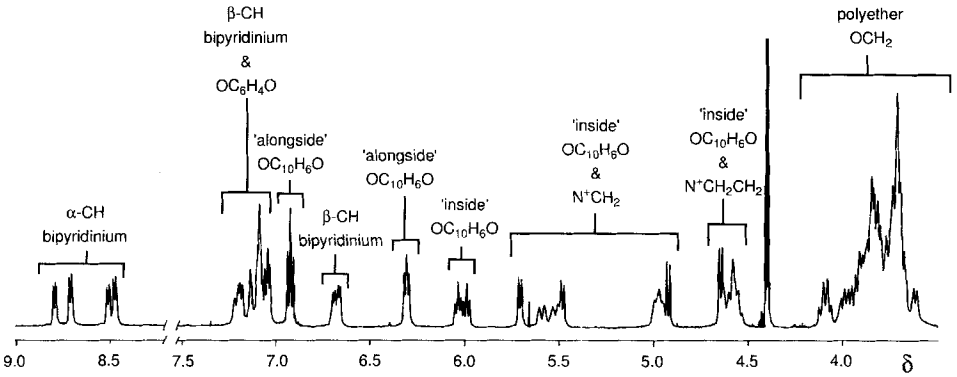

Figure 8. ^{1}H NMR spectrum (500 MHz) of the [3]catenane **6a**·4PF$_6$ (238 K, CD_3COCD_3/CD_3NO_2 (4:1, *v*/*v*)). Spectral assignments are summarized.

Portions of the low-field region of the NOESY/EXSY matrix are shown in Figure 10. Two—unequally intense—pairs of doublets attributable to the α-CH bipyridinium protons of isomer **A** (δ = 8.79 and 8.51) and isomer **B** (δ = 8.71 and 8.47) are clearly re-

Table 3. ^{1}H NMR Chemical shift data (δ values) for the [3]catenanes **6a**·4PF$_6$, **6b**·4PF$_6$, and **6c**·4PF$_6$.
a) Tetracationic cyclophane component.

Compound	Bipyridinium Unit α-CH	β-CH	C_6H_4	Spacer CH_2N^+	CH_2O
6a·4PF$_6$ (**A**) [a]	8.79 [d], 8.51 [e]	7.16–7.24 [d]	7.08–7.10	4.89–5.02	4.52–468
		6.69 [e]	7.11–7.14	5.46–5.61	
6a·4PF$_6$ (**B**) [a]	8.71 [d], 8.47 [e]	7.08–7.10 [d]	7.08–7.10	4.89–5.02	4.52–4.68
		6.66 [e]	7.16–7.24	5.46–5.61	
6b·4PF$_6$ [b]	8.74	7.63	6.81	5.01	4.41
6c·4PF$_6$ [c]	8.96	7.87	6.88	5.00–5.06	4.41–4.47

b) Aromatic unit of the macrocyclic polyether component.

Compound	1,5-Dioxynaphthalene Ring System H-4/8	H-3/7	H-2/6	Hydroquinone Ring
6a·4PF$_6$ (**A**) [a]	7.14 [f], 5.02 [g]	7.03 [f], 6.08 [g]	6.41 [f], 5.58 [g]	–
6a·4PF$_6$ (**B**) [a]	7.06 [f], 4.65 [g]	6.93 [f], 6.03 [g]	6.29 [f], 5.71 [g]	–
6b·4PF$_6$ [b]	–	–	–	5.44 [h]
6c·4PF$_6$ [c]	–	–	–	4.91 [i]

[a] At 500 MHz in CD_3COCD_3/CD_3NO_2 (4/1, *v*/*v*) at 238 K. [b] At 300 MHz in CD_3COCD_3 at 298 K. [c] At 300 MHz in CD_3CN at 298 K. [d] Protons ▾ on the bipyridinium units as defined in Figure 10. [e] Protons ▲ on the bipyridinium units as defined in Figure 10. [f] Protons on the aromatic ring system of the crown ether component located "outside" the cavity of the tetracationic cyclophane. [g] Protons on the aromatic ring system of the crown ether component located "inside" the cavity of the tetracationic cyclophane. [h] Protons on the hydroquinone ring located "outside" the cavity of the tetracationic cyclophane. [i] Averaged resonance for the fast exchange between the hydroquinone ring protons of the crown ether component located "inside" and "outside" the cavity of the tetracationic cyclophane.

0947-6539/97/0305-0792 $ 17.50+.50/0 Chem. Eur. J. 1997, 3, No. 5

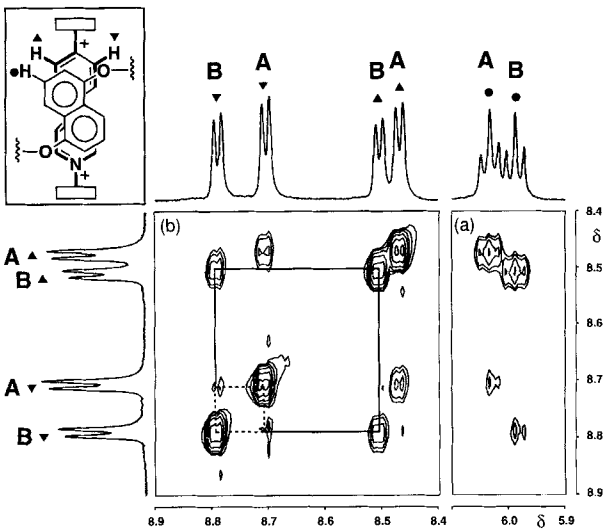

Figure 10. Portions of the 500 MHz 2D NOESY spectrum (238 K) of the [3]catenane **6a**·4PF$_6$. a) Matrix crosspeaks defining the disposition of the α-CH bipyridinium protons for both isomers **A** and **B** (▲ and ▼ denote the nearest and farthest environments, respectively, with respect to the H-3/7 protons, labeled ●, on the included 1,5-dioxynaphthalene ring systems). b) Matrix crosspeaks indicating chemical exchange between α-CH proton environments for both isomers **A** and **B**.

solved. Cross-peaks defining the disposition of each member of the α-CH bipyridinium proton pairs with respect to the proximal, included, C_{2h} symmetric, 1,5-dioxynaphthalene unit, that is, cross-peaks linking each doublet with the apparent triplet assignable to the H-3/7 protons on the 1,5-dioxynaphthalene residue are well-defined in the contour map (Figure 10a). Site-exchange between all four α-CH bipyridinium proton environments is evident from inspection of Figure 10b. Clearly, site-exchange *within* each isomer (solid lines) is occurring more rapidly than site-exchange *between* the isomers **A** and **B** (dashed lines), as indicated by the integrated intensities of the related cross-peaks.

In order to delineate the processes affecting the site-exchange of the α-CH bipyridinium protons between their four environments, we conducted lineshape analyses[18] of the low-field region of a series of 400 MHz ^{1}H NMR spectra recorded on a CD_3COCD_3/CD_3NO_2 (4:1, *v*/*v*) solution of the [3]catenane **6a**·4PF$_6$ over a temperature range of 246 to 314 K. Site-exchange of this type has been observed previously in catenanes incorporating the cyclobis(paraquat-4,4′-biphenylene) tetracation and crown ether components containing the 1,5-dioxynaphthalene ring system.[13] In these systems, the process associated with site-exchange cannot be defined unambiguously. Site-exchange of the α-CH bipyridinium protons can be achieved through process I and/or II, as illustrated in Scheme 2. In **6a**·4PF$_6$, however, process I and II—that is, dissociation of the included 1,5-dioxynaphthalene residues, followed by either the rotation (process I) of the bipyridinium unit about its long axis or reorientation (process II) of the 1,5-dioxynaphthalene residue, prior to re-association of the π-electron rich donor—lead to discrete site-exchange: process I leads to exchange *within* one isomer, while process II leads to the interconversion between isomers and hence exchange *between* isomers. The series of equilibria associated with the exchange pathways is shown in Scheme 3.

The equilibrium constants for the interconversion of the D_2 and C_{2h} isomers **A** and **B**, respectively, were calculated directly

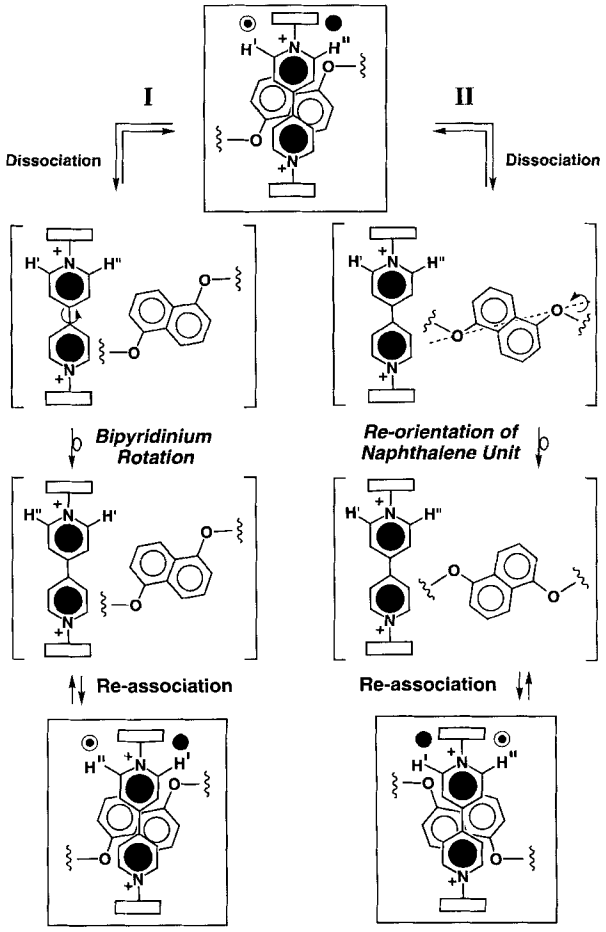

Scheme 2. Schematic representation of the two possible dynamic processes that account for the averaging of the chemical environments of the α-CH bipyridinium protons in the tetracationic cyclophane components of catenanes derived from crown ethers containing 1,5-dioxynaphthalene residues. The filled circles and the circles with a dot at their center stand for α-CH bipyridinium proton environments nearest and farthest, respectively, to the H-3/7 protons of the 1,5-dioxynaphthalene ring systems included "inside" the cavity of the tetracationic cyclophane. H′ and H″ denote the frequency labeling of the α-CH bipyridinium protons.

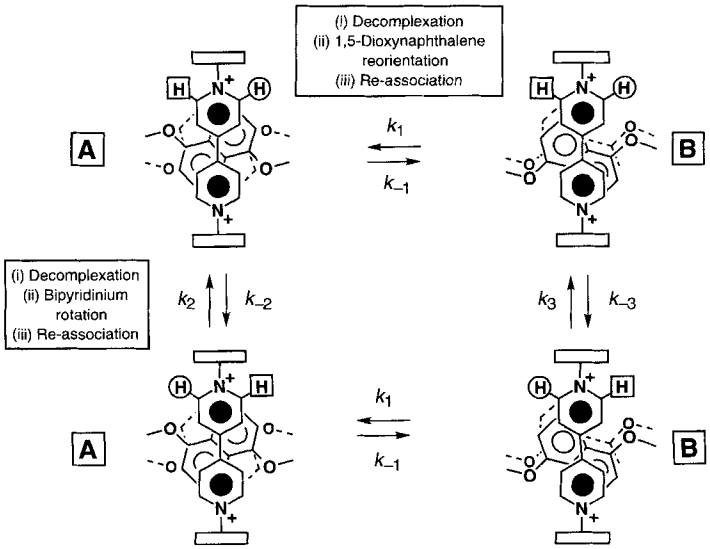

Scheme 3. Kinetic scheme outlining the dynamic processes occurring in the [3]catenane **6a**·4PF$_6$; k_1 and k_{-1} are the rate constants associated with the site-exchanges between the isomers **A** and **B**. k_2, k_{-2} and k_3, k_{-3} are the rate constants associated with the site-exchanges within "isomer" **A** and within isomer **B**, respectively.

from the integral intensities of appropriately well-dispersed resonances at temperatures where the site-exchange rates were slow on the 400 MHz ^{1}H NMR timescale. The K_{eq} values and the associated free energies (ΔG°) are listed in Table 4. From the temperature dependence of K_{eq} (Figure 11), values of ΔH° equal to -1.2 ± 0.2 kcal mol^{-1} and of ΔS° equal to -5 ± 1 cal mol^{-1} K^{-1} were calculated for the interconversion of **A** and **B**. These data show that the position of the equilibrium between the D_2 and C_{2h} isomers is entropically driven over the temperature range investigated.

Table 4. Equilibrium constants K_{eq} [a] and related free energies ΔG° at various temperatures associated with the equilibrium between the isomers **A** and **B** of the [3]catenane **6a**·4PF$_6$.

T (K)	K_{eq} [a]	ΔG° (kcal mol^{-1})
220	1 ± 0.05	0 ± 0.02
238	0.83 ± 0.04	0.08 ± 0.03
246	0.79 ± 0.04	0.12 ± 0.02
255	0.68 ± 0.04	0.19 ± 0.04
264	0.66 ± 0.04	0.21 ± 0.04
273	0.58 ± 0.03	0.29 ± 0.03

[a] The equilibrium constant is defined by the equation: K_{eq} = [isomer **A**]/[isomer **B**].

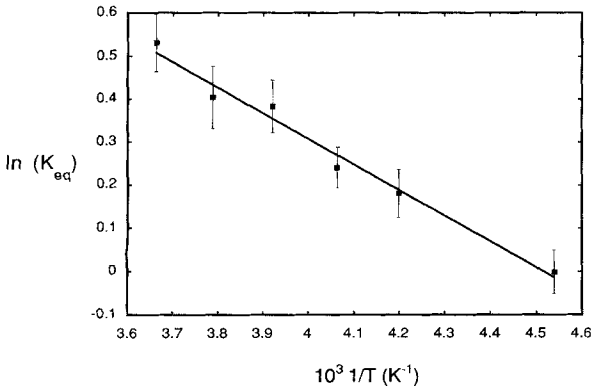

Figure 11. Arrhenius plot of the equilibrium constant K_{eq} between the two isomers **A** and **B** of **6a**·4PF$_6$, where K_{eq} = [isomer **A**]/[isomer **B**]. The curve fit was obtained by employing the linear regression method (slope: -0.596 K, intercept: 2.69, $R = 0.991$).

The values of the site-exchange rate constants k_1, k_2, and k_3 (Scheme 3) calculated from lineshape analyses,[11,8] the related free energies of activation ($\Delta G_1^{\ddagger}$, $\Delta G_2^{\ddagger}$, and $\Delta G_3^{\ddagger}$) and the values of k_{-1} and $\Delta G_{-1}^{\ddagger}$, derived from $\Delta G_1^{\ddagger}$ and ΔG°, are listed in Table 5 and illustrated in Figure 12. Enthalpies and entropies of activation ($\Delta H^{\ddagger}$ and $\Delta S^{\ddagger}$) were derived from the free energies of activation ($\Delta G^{\ddagger}$) and are recorded in Table 6.

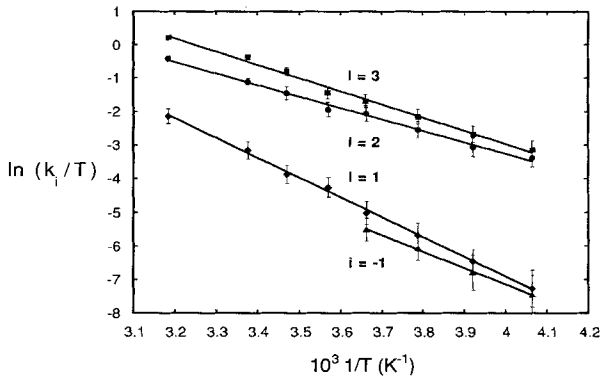

Figure 12. Eyring plot of the rate constants for the exchanges: ■ within isomer **B** ($i = 3$, slope: -3.9 K, intercept: 12.8), ● within isomer **A** ($i = 2$, slope: -3.4 K, intercept: 10.4), ◆ between isomers **A** and **B** (**B** → **A**, $i = 1$, slope: -5.9 K, intercept: 16.7), and ▲ between isomers **A** and **B** (**A** → **B**, $i = -1$, slope: -4.9 K, intercept: 12.5) in the [3]catenane **6a**·4PF$_6$. The curve fit was obtained by employing the linear regression method ($R = 0.999$ for $i = 1$, $R = 0.996$ for $i = 2$, $R = 0.996$ for $i = 3$, $R = 0.999$ for $i = -1$).

Table 6. Enthalpies ($\Delta H_i^{\ddagger}$) and entropies($\Delta S_i^{\ddagger}$) of activation associated with the dynamic processes occurring in **6a**·4PF$_6$ derived from the Eyring plot Figure 12.

	$i=1$	$i=2$	$i=3$	$i=-1$
$\Delta H_i^{\ddagger}$ (kcal mol^{-1})	11.7 ± 0.3	6.9 ± 0.2	7.8 ± 0.2	10.5 ± 0.3
$\Delta S_i^{\ddagger}$ (cal mol^{-1} K^{-1})	$-14\ \pm2$	$-26\ \pm3$	$-22\ \pm2$	$-19\ \pm3$

It is noteworthy that the data could not be matched with a kinetic scheme employing only four rate constants. Of course, the rate constants calculated herein represent the rate-determining step for the four three-step processes (dissociation, rotation, and reassociation) affecting the site-exchange of the α-CH bypiridinium protons between four environments (Scheme 2). It is reasonable to expect that the rate-determining step would be the initial step—dissociation of the 1,5-dioxynaphthalene ring system from the cavity of the tetracation—as this step requires the disruption, or at least the partial disruption, of several noncovalent bonding interactions. The dissociation should therefore be more energetically demanding than any subsequent σ-

Table 5. Rate constants k_1, k_2, k_3, and k_{-1} and related free energies of activation $\Delta G_1^{\ddagger}$, $\Delta G_2^{\ddagger}$, $\Delta G_3^{\ddagger}$, and $\Delta G_{-1}^{\ddagger}$ associated with the dynamic processes depicted in Scheme 3 occurring in the [3]catenane **6a**·4PF$_6$, as calculated by lineshape analysis at various temperature.

T (K)	k_1 (s^{-1})	k_2 (s^{-1})	k_3 (s^{-1})	k_{-1} [a] (s^{-1})	$\Delta G_1^{\ddagger}$ (kcal mol^{-1})	$\Delta G_2^{\ddagger}$ (kcal mol^{-1})	$\Delta G_3^{\ddagger}$ (kcal mol^{-1})	$\Delta G_{-1}^{\ddagger}$ [a] (kcal mol^{-1})
246	0.17 ± 0.07	8.4 ± 2.0	10.7 ± 2.5	0.14 ± 0.06	15.2 ± 0.2	13.3 ± 0.1	13.2 ± 0.1	15.3 ± 0.2
255	0.40 ± 0.12	12.1 ± 2.9	17.9 ± 3.9	0.28 ± 0.11	15.3 ± 0.2	13.6 ± 0.1	13.4 ± 0.1	15.5 ± 0.2
264	0.90 ± 0.27	21.1 ± 4.6	31.0 ± 6.2	0.61 ± 0.18	15.5 ± 0.2	13.8 ± 0.1	13.6 ± 0.1	15.7 ± 0.2
273	1.81 ± 0.52	35.0 ± 7.0	51.0 ± 9.1	1.11 ± 0.32	15.6 ± 0.2	14.0 ± 0.1	13.8 ± 0.1	15.9 ± 0.2
280	4.00 ± 1.00	40.4 ± 7.7	67.1 ± 11.1	–	15.6 ± 0.15	14.3 ± 0.1	14.0 ± 0.1	–
288	6.07 ± 1.46	68.0 ± 11.6	130 ± 14	–	15.8 ± 0.15	14.4 ± 0.1	14.1 ± 0.1	–
295	12.8 ± 3.0	98.4 ± 9.2	207 ± 15	–	15.9 ± 0.1	14.7 ± 0.1	14.2 ± 0.1	–
314	37.0 ± 7.0	208 ± 16	392 ± 25	–	16.2 ± 0.1	15.1 ± 0.1	14.7 ± 0.1	–

[a] Only four data points were available in the calculation of $\Delta G_{-1}^{\ddagger}$ and k_{-1} from ΔG° and $\Delta G_{-1}^{\ddagger}$.

0947-6539/97/0305-0794 $ 17.50+.50/0 Chem. Eur. J. 1997, 3, No. 5

bond rotations. The observation of two distinct site-exchange rate constants, namely, k_2 and k_3, for the α-CH bipyridinium protons within each of the isomers **A** and **B** is in accordance with this proposal. If the rate of site-exchange was dependent upon the rate of the rotation of the bipyridinium units around their N···N axes, then we would expect k_2 and k_3 to be equal. A comparison of the values observed for k_1 and k_{-1} with those obtained for k_2 and k_3 suggests that the 1,5-dioxynaphthalene ring system must exit from the cavity of the tetracationic cyclophane to a far greater extent in order to allow its reorientation to take place, compared with how far it has to exit to enable the rotation of the bipyridinium units. It would appear that the two included 1,5-dioxynaphthalene ring systems are oscillating continuously within the center of the cavity, such that a partial dissociation of one 1,5-dioxynaphthalene ring system allows the adjacent bipyridinium units to rotate about their long axes, whereas a complete dissociation is presumably necessary to allow the 1,5-dioxynaphthalene unit to rotate about its O···O axis.

The ^{1}H NMR spectrum of the [3]catenane **6b**·4PF$_6$ at room temperature appears uniformly sharp and can be readily assigned (Table 3). On cooling down a solution of **6b**·4PF$_6$ in CD_3COCD_3 (400 MHz), we observed the separation of the signal corresponding to the hydroquinone ring protons of the crown ether component into two signals associated with "inside" and "alongside" environments for these rings. The free energy of activation, $\Delta G_c^{\ddagger}$ (T_c = 291 K at 400 MHz), associated with this site-exchange process[21,22] is 13.0±0.2 kcal mol^{-1}. Further cooling of the solution of **6b**·4PF$_6$ results in the separation of the resonances corresponding to the β-CH bipyridinium protons and the resonances associated with the hydroquinone ring protons located "inside" the cavity of the tetracation. The lower temperature spectrum (188 K at 400 MHz) is consistent with a scenario in which the so-called "rocking" motion[10] of the hydroquinone rings included "inside" the cavity of the tetracation becomes slow on the 400 MHz ^{1}H NMR timescale, a process previously observed[10] in other [2]catenanes. The activation energy, $\Delta G_c^{\ddagger}$ (T_c = 212 K at 400 MHz), associated with this "rocking" process[21,23] is 9.5±0.2 kcal mol^{-1}. The slowing down of the rocking of the hydroquinone rings should ultimately lead to the emergence of two D_2 and C_{2h} isomers, analogous to those observed in **6a**·4PF$_6$. However, the interconversion between these isomers would presumably require considerably less energy than the interconversion of the isomers **A** and **B** in **6a**·4PF$_6$.

The spectra of the [3]catenane **6c**·4PF$_6$ recorded in CD_3COCD_3 at 400 MHz reveal that the hydroquinone rings of the crown ether component reside, on average, within the cavity of the tetracationic cyclophane, over the temperature range from 193 to 313 K. At temperatures below 270 K, the spectrum broadens, and the signals corresponding to hydroquinone ring protons of the crown ether component separate in accordance with the slowing down of the rocking motion, as previously observed for the [3]catenane **6b**·4PF$_6$. The activation energy, $\Delta G_c^{\ddagger}$ (T_c = 197 K at 400 MHz), associated with this process[21,24] in CD_3COCD_3 is 9.5±0.2 kcal mol^{-1}, a value that is, not surprisingly, similar to the one observed in the [3]catenane **6b**·4PF$_6$.

Conclusion

The preparation and characterization of three new [3]catenanes **6a**·4PF$_6$, **6b**·4PF$_6$, and **6c**·4PF$_6$ has enlarged the range of interlocked structures attainable through self-assembly methodologies and could ultimately lead to the realization of even higher order catenanes. The solid-state structures of the three [3]catenanes reveal that their structures are maintained as a result of a wide range of noncovalent bonding interactions, including π–π interactions, [CH···O] hydrogen bonds and [CH···π] interactions. Moreover, the elucidation of the dynamics of the solution-state structures of these molecules by ^{1}H NMR spectroscopy has revealed a novel type of isomerism that had not been observed previously in similar catenated compounds. At low temperature, **6a**·4PF$_6$, **6b**·4PF$_6$, and **6c**·4PF$_6$ in solution exist in two isomeric forms, possessing either C_{2h} or D_2 symmetries, which equilibrate slowly on the 400 MHz ^{1}H NMR timescale. Lineshape analyses of the ^{1}H NMR spectra of **6a**·4PF$_6$ have afforded kinetic parameters previously unattainable using either coalescence or line broadening methods. The free energies of activation at 298 K are, for the exchange between isomers, ca. 16 kcal mol^{-1}, and for the exchange within isomers (i.e., rotation of the bipyridinium units about their long axes), ca. 14.5 kcal mol^{-1}. It is now clear that the disruption of noncovalent bonding interactions—namely, a combination of π–π interactions, edge-to-face T-type interactions, and hydrogen-bonding interactions—is more energy demanding than are rotations about σ-bonds in these types of molecules. This research has provided us with a much better understanding of the behavior of bipyridinium-based interlocked molecules in solution, and is aimed, ultimately, at helping synthetic chemists in the design of new generations of molecular assemblies and supramolecular arrays.

Experimental Section

Materials and Methods: Chemicals, including hydroquinone bis(2-hydroxyethyl) ether, were purchased from Aldrich and used without further purification. Solvents were either used as purchased or dried (DMF from KOH, MeCN from CaH_2), according to procedures described in the literature.[25] The reactions requiring ultrahigh pressure were carried out in a Teflon vessel using a custom-built ultrahigh-pressure press, manufactured by PSIKA Pressure Systems of Glossop, UK. Thin layer chromatography (TLC) was carried out using aluminum sheets precoated with silica gel 60 F (Merck 5554). The plates were inspected by UV light and developed with a dilute solution of I_2 in $CHCl_3$. Column chromatography was carried out using silica gel 60 F (Merck 9385, 230–400 mesh). Melting points were determined on an Electrothermal 9200 apparatus and are not corrected. Low-resolution mass spectra were performed using a Kratos Profile spectrometer, operating in electron impact (EIMS) mode. Fast-atom bombardment mass spectra (FABMS) were recorded on a Kratos MS 80 spectrometer, operating at 8 keV using a xenon primary atom beam. The matrix used was 3-nitrobenzyl alcohol (NOBA). Liquid secondary-ion mass spectra (LSI-MS) were recorded on a VG ZabSpec mass spectrometer, using a *m*-nitrobenzyl alcohol matrix and a scan speed of 10 s per decade. X-Ray crystallography and ^{1}H NMR spectroscopy are discussed in separate paragraphs at the end of this Experimental Section.

Hydroquinone bis(2-bromoethyl) ether (3):[19] Bromine (16.0 g, 0.10 mol) was added to a mechanically stirred suspension of Ph_3P (26.6 g, 0.1 mol) in dry MeCN (100 mL) at 5 °C at such a rate that the supernatant solution remained colorless. The solution was then allowed to warm up to room temperature and powdered hydroquinone bis(2-hydroxyethyl) ether (9.9 g, 0.05 mol) was added in one portion. After 15 min, total dissolution of the precipitate had

occurred, and after 1 h, a new precipitate started to form. After yet another 2 h, the reaction mixture was filtered, and the filtrate evaporated in vacuo to yield hydroquinone bis(2-bromoethyl) ether **3** as a white solid which was recrystallized from MeOH (6.8 g, 42.0%): m.p. 111–113 °C; ^{1}H NMR (300 MHz, $CDCl_3$, 298 K): $\delta = 6.88$ (s, 4H, aromatic protons), 4.26 (t, $J = 7.5$ Hz, 4H, OCH_2), 3.62 (t, $J = 7.5$ Hz, 4H, CH_2Br); ^{13}C NMR (75.5 MHz, $CDCl_3$, 298 K): $\delta = 153.9, 117.0, 69.8, 31.6$; MS (70 eV, EI): *m/z* (%) = 324 (100) $[M]^+$; HREIMS calcd. for $C_{10}H_{12}O_2{}^{79}Br_2$ $[M]^+$: *m/z* 321.92040; found: *m/z* 321.92078.

Dicationic Salt 4·2PF$_6$:[19] During seven days, the dibromide **3** (1.05 g, 3.2 mmol) was added portionwise three times a day (50 mg per portion) to a refluxing solution of 4,4′-bipyridine (5.05 g, 32.4 mmol) in dry MeCN (100 mL) under nitrogen. The reaction mixture was maintained under reflux for a further 48 h before it was allowed to cool down to room temperature. The greenish brown precipitate was filtered, dissolved in a mixture of Me_2CO and H_2O, and purified by column chromatography [SiO_2/MeOH–2N aqueous NH_4Cl–$MeNO_2$ (7:2:1)] to yield, after counterion exchange, **4**·2PF$_6$, as a yellow solid (1.3 g, 50%): m.p. > 250 °C; ^{1}H NMR (300 MHz, CD_3CN, 298 K): $\delta = 9.42$ (d, $J = 7.0$ Hz, 4H, pyridinium α-CH), 8.87 (d, $J = 6.0$ Hz, 4H, pyridine α-CH), 8.72 (d, $J = 7.0$ Hz, 4H, pyridinium β-CH), 7.99 (d, $J = 6.0$ Hz, 4H, pyridine β-CH), 6.92 (s, 4H, hydroquinone), 5.32 (t, $J = 5.5$ Hz, 4H. CH_2N^+), 4.65 (t, $J = 5.5$ Hz, 4H, OCH_2); ^{13}C NMR (75.5 MHz, CD_3CN, 298 K): $\delta = 155.7, 153.6, 152.2, 146.6, 142.1, 127.0, 123.2, 116.8, 67.5, 61.7$; FABMS: *m/z*: 621 $[M - PF_6]^+$; HRLSIMS calcd. for $C_{30}H_{28}O_2N_2PF_6$ $[M - PF_6]^+$: *m/z* 621.18541; found: *m/z* 621.18685.

[3]Catenane 6a·4PF$_6$:

Method A: The dicationic salt **4**·2PF$_6$ (46.0 mg, 0.06 mmol), the dibromide **3** (19.4 mg, 0.06 mmol), and 1,5-DNP38C10 (**5a**; 95.5 mg, 0.15 mmol) were dissolved in dry DMF (15 mL). The solution was transferred to a Teflon high-pressure reaction vessel, which was compressed at 12 kbar for 5 d at 20 °C. Et_2O (200 mL) was then added to the mixture and the resulting precipitate collected by filtration and purified by column chromatography [SiO_2/MeOH–2N aqueous NH_4Cl–$MeNO_2$ (7:2:1)] affording, after counterion exchange, **6a**·4PF$_6$ as a deep purple solid (51.0 mg, 34%): m.p. > 250 °C; ^{1}H NMR (isomer **A**/isomer **B** : 56/44, 500 MHz, CD_3COCD_3/CD_3NO_2 : 4/1, 238 K): $\delta = 8.79$ (d, $J = 6.1$ Hz, **A**: 4H), 8.71 (d, $J = 6.7$ Hz, **B**: 4H), 8.51 (d, $J = 6.7$ Hz, **A**: 4H), 8.47 (d, $J = 6.7$ Hz, **B**: 4H), 7.24–7.16 (m, $J = 6.1$ Hz, **A**: 4H, **B**: 4H), 7.14 (d, $J = 8.1$ Hz, **A**: 4H), 7.14–7.11 (m, **A**: 4H), 7.10–7.08 (m, $J = 6.7$ Hz, **A**: 4H, **B**: 8H), 7.06 (d, $J = 4.4$ Hz, **B**: 4H), 7.03 (d, $J = 4.2$ Hz, **A**: 4H), 6.93 (t, $J = 7.8$ Hz, **B**: 4H), 6.69 (d, $J = 6.7$ Hz, **A**: 4H), 6.66 (d, $J = 6.7$ Hz, **B**: 4H), 6.41 (d, $J = 4.4$ Hz, **A**: 4H), 6.29 (d, $J = 4.2$ Hz, **B**: 4H), 6.08 (t, $J = 7.9$ Hz, **A**: 4H), 6.03 (t, $J = 8.1$ Hz, **B**: 4H), 5.71 (d, $J = 7.8$ Hz, **B**: 4H), 5.61–5.46 (m, **A**: 4H, **B**: 4H), 5.58 (d, $J = 7.9$ Hz, **A**: 4H), 5.02–4.89 (m, **A**: 4H, **B**: 4H), 5.02 (d, $J = 8.1$ Hz, **A**: 4H), 4.65 (d, $J = 8.1$ Hz, **B**: 4H), 4.68–4.52 (m, **A**: 8H, **B**: 8H), 4.24–3.68 (m, **A**: 64H, **B**: 64H); FABMS *m/z* 2347 $[M - PF_6]^+$, 2202 $[M - 2PF_6]^+$, 2057 $[M - 3PF_6]^+$; HRLSIMS calcd. for $C_{112}H_{128}N_4O_{24}F_{12}P_2$ $[M - 2PF_6]^+$: *m/z* 2202.8202; found: *m/z* 2202.8163. Single crystals, suitable for X-ray crystallography, were grown by slow evaporation of a solution of **6a**·4PF$_6$ in CD_3COCD_3.

Method B: The dicationic salt **4**·2PF$_6$ (46.0 mg, 0.06 mmol), the dibromide **3** (19.4 mg, 0.06 mmol), and 1,5-DNP38C10 (**5a**; 95.5 mg, 0.15 mmol) were dissolved in dry DMF (15 mL). The solution was stirred for 9 weeks at room temperature prior to the addition of Et_2O (200 mL). The resulting precipitate was collected by filtration and then purified by column chromatography [SiO_2/MeOH–2N aqueous NH_4Cl–$MeNO_2$ (7:2:1)] affording, after counterion exchange, **6a**·4PF$_6$ as a deep purple solid (1.6 mg, 1.1%) with identical physical properties to those for a sample obtained by method A.

[3]Catenane 6b·4PF$_6$:

Method A: The dicationic salt **4**·2PF$_6$ (46.0 mg, 0.06 mmol), the dibromide **3** (19.4 mg, 0.06 mmol), and BPP34C10 (**5b**; 80.5 mg, 0.15 mmol) were dissolved in dry DMF (15 mL). The solution was transferred to a Teflon high-pressure reaction vessel which was compressed at 12 kbar for 5 d at 20 °C. Et_2O (200 mL) was then added to the mixture, and the resulting precipitate collected by filtration and purified by column chromatography [SiO_2/MeOH–2N aqueous NH_4Cl–$MeNO_2$ (7:2:1)] affording, after counterion exchange, **6b**·4PF$_6$ as a deep purple solid (51.0 mg, 31%): m.p. > 250 °C; ^{1}H NMR (300 MHz, CD_3COCD_3, 25 °C): $\delta = 8.74$ (d, $J = 7.0$ Hz, 8H), 7.63 (d, $J = 7.0$ Hz, 8H), 6.81 (s, 8H), 5.44 (bs, 16H), 5.01 (m, 8H), 4.41 (bs, 8H), 3.71-3.77 (m, 32H), 3.51 (m, 16H), 3.11 (m, 16H); FABMS *m/z* 2147 $[M - PF_6]^+$, 2002 $[M - 2PF_6]^+$, 1857 $[M - 3PF_6]^+$; HRLSIMS calcd. for $C_{96}H_{120}N_4O_{24}F_{18}P_3$ $[M - PF_6]^+$: *m/z* 2147.7218; found: *m/z* 2147.7248; $C_{96}H_{120}N_4O_{24}P_4F_{24}$ (2147.7): calcd C 50.27, H 5.27, N 2.44; found C 50.43, H 5.67, N 2.66. Single crystals, suitable for X-ray crystallography, were grown by vapor diffusion of iPr_2O into a solution of **6b**·4PF$_6$ in MeCN.

Method B: The dicationic salt **4**·2PF$_6$ (100.0 mg, 0.13 mmol), the dibromide **3** (42.0 mg, 0.13 mmol), and BPP34C10 (**5b**; 175.0 mg, 0.32 mmol) were dissolved in dry MeCN (25 mL). The solution was stirred for 9 weeks at room temperature prior to the addition of Et_2O (200 mL). The resulting precipitate was collected by filtration and then purified by column chromatography [SiO_2/MeOH–2N aqueous NH_4Cl–$MeNO_2$ (7:2:1)] affording, after counterion exchange, **6b**·4PF$_6$ as a deep purple solid (2.5 mg, 0.8%) with identical physical properties to those for a sample obtained by method A.

[3]Catenane 6c·4PF$_6$: The dicationic salt **4**·2PF$_6$ (13.1 mg, 0.043 mmol), the dibromide **3** (5.5 mg, 0.017 mmol), and **5c** (26.0 mg, 0.017 mmol) were dissolved in dry DMF (3 mL). The solution was transferred to a Teflon high-pressure reaction vessel, which was compressed at 12 kbar for 5 d at 20 °C. Et_2O (50 mL) was then added to the mixture, and the resulting precipitate collected by filtration and purified by column chromatography [SiO_2/MeOH–2N aqueous NH_4Cl–$MeNO_2$ (7:2:1)] affording, after counterion exchange, **6c**·4PF$_6$ as a red solid (13.9 mg, 33%): m.p. > 250 °C; ^{1}H NMR (300 MHz, CD_3CN, 25 °C): $\delta = 8.96$ (d, $J = 7.0$ Hz, 8H), 7.87 (d, $J = 7.0$ Hz, 8H), 6.88 (s, 8H), 5.00–5.06 (m, 8H), 4.91 (s, 8H), 4.41–4.47 (m, 8H), 3.66–3.82 (m, 40H), 3.53–3.60 (m, 8H), 3.43–3.49 (m, 8H), 2.92–2.98 (m, 8H); FABMS m/z 2436 $[M]^+$, 2291 $[M - PF_6]^+$, 2146 $[M - 2PF_6]^+$, 2001 $[M - 3PF_6]^+$; HRLSIMS calcd. for $C_{96}H_{120}N_4O_{24}F_{12}P_2$ $[M - 2PF_6]^+$: *m/z* 2146.6894; found: *m/z* 2146.6822. Single crystals, suitable for X-ray crystallography, were grown by vapor diffusion of iPr_2O into a solution of **6c**·4PF$_6$ in MeCN.

X-Ray Crystallography: Table 7 provides a summary of the crystal data, data collection, and refinement parameters for complexes **6a**·4PF$_6$, **6b**·4PF$_6$, and **6c**·4PF$_6$. All the structures were solved by direct methods and were refined by full-matrix least-squares based on F^2. Each of the three [3]catenane complexes were well-defined and all their non-hydrogen atoms were refined anisotropically. Structures **6a**·4PF$_6$ and **6c**·4PF$_6$ contain disordered PF_6^- anions, which were in each case resolved into alternate, partial occupancy orientations, the major occupancy components of which were refined anisotropically. In **6b**·4PF$_6$, the PF_6^- anions showed no disorder and were refined anisotropically. All of the structures contain multiple included solvent molecules—in **6a**·4PF$_6$ and **6b**·4PF$_6$, these were ordered, full occupancy, and were refined anisotropically, whereas for **6c**·4PF$_6$, they were disordered, of partial occupancy and, refined isotropically. All of the C–H hydrogen atoms in each of the three structures were placed in calculated positions, assigned isotropic thermal parameters, $U(H) = 1.2\,U_{eq}(C)$ [$U(H) = 1.5\,U_{eq}(C\text{–Me})$], and allowed to ride on their parent atoms. Computations were carried out using the SHELXTL PC program system.[26]

The crystallographic data (excluding structure factors) for the structures reported in Table 7 have been deposited with the Cambridge Crystallographic Data Centre as supplementary publication number CCDC-1220-50. Copies of the data can be obtained free of charge on application to The Director, CCDC, 12 Union Road, Cambridge, CB121EZ, UK (Fax: Int. code +(1223)336-033; e-mail: deposit@chemcrys.cam.ac.uk).

^{1}H NMR Spectroscopy: ^{1}H NMR spectra were recorded on Bruker AC300, AMX400, and AMX500 spectrometers. Chemical shifts are referenced to solvent resonances. Probe temperatures were measured using a Comark-type K thermocouple. The NOESY/EXSY spectrum was recorded by using 480 increments of 32 transients. τ_{mix} was set to 400 ms. Cosine weighting functions were applied in both dimensions prior to fourier transformation. lineshape analyses were conducted using the DNMR5 program[18]. The natural linewidth in the absence of exchange, $\omega_{1/2}$, a quantity necessary for the simulation of the resonances of the α-CH bipyridinium protons, is not directly accessible because the atoms in the [3]catenane **6a**·4PF$_6$ are necessarily undergoing various site-exchange processes, over the temperature range of interest. An estimate of $\omega_{1/2}$ was calculated from the corresponding resonances in a second series of spectra recorded under identical conditions on a solution of the fluorinated analogue of **6a**·4PF$_6$, i.e., **6c**·4PF$_6$. Site-exchange involving the α-CH bipyridinium protons in the [3]catenane **6c**·4PF$_6$ is slow on the ^{1}H NMR timescale (400 MHz) over the temperature range of interest.

0947-6539/97/0305-0796 $ 17.50+.50/0 Chem. Eur. J. 1997, 3, No. 5

Table 7. Crystal data, data collection, and refinement parameters [a].

	6a·4PF$_6$	**6b**·4PF$_6$	**6c**·4PF$_6$
empirical formula	$C_{112}H_{128}N_4O_{24}\cdot 4PF_6$	$C_{96}H_{120}N_4O_{24}\cdot 4PF_6$	$C_{96}H_{112}N_4O_{24}F_8\cdot 4PF_6$
solvent	6Me$_2$CO	12MeCN	7MeCN
M_r	2842.5	2786.5	2725.2
color, habit	red blocks	orange-red platy needles	red prisms
crystal size/mm	0.27 × 0.20 × 0.13	0.67 × 0.27 × 0.07	0.50 × 0.33 × 0.23
crystal system	triclinic	triclinic	monoclinic
space group	$P\bar{1}$	$P\bar{1}$	$P2_1/n$
T/K	293	200	203
a/Å	14.476(4)	14.126(8)	13.813(1)
b/Å	14.978(4)	14.820(10)	35.480(2)
c/Å	16.643(5)	18.610(16)	14.382(1)
α/°	73.26(2)	76.92(6)	–
β/°	84.32(2)	83.92(6)	101.92(1)
γ/°	84.75(2)	64.12(5)	–
V/Å^3	3431(2)	3414(4)	6896.7(7)
Z	1 [b]	1 [b]	2 [b]
ρ/gcm^{-3}	1.376	1.355	1.312
$F(000)$	1488	1456	2820
μ/mm^{-1}	1.430	1.418	1.468
2θ Range/°	5.6–120.0	4.8–110.0	5.0–110.0
independent reflections	10187	8566	7232
observed reflections, $\lvert F_o\rvert > 4\sigma(\lvert F_o\rvert)$	6581	7182	3750
number of parameters	944	848	836
R_1 [c]	0.069	0.055	0.153
wR_2 [d]	0.173	0.142	0.385
weighting factors a, b [e]	0.099, 2.691	0.084, 3.448	0.281, 46.165
largest difference peak, hole/e Å^{-3}	0.32, −0.32	0.49, −0.36	0.77, −0.57

[a] Details in common: graphite monochromated $Cu_{K\alpha}$ radiation, ω scans, Siemens P4 rotating anode diffractometer, refinement based on F^2. [b] The molecule has crystallographic C_i symmetry. [c] $R_1 = \sum||F_o| - |F_c||/\sum|F_o|$. [d] $wR_2 = \sqrt{\{\sum[w(F_o^2 - F_c^2)^2]/\sum[w(F_o^2)^2]\}}$. [e] $w^{-1} = \sigma^2(F_o^2) + (aP)^2 + bP$.

Acknowledgements: This research was supported by the Engineering and Physical Sciences Research Council as well as by Merck Sharp & Dohme in the UK, and by the Ministère de la Recherche et de l'Enseignement Supérieur in France. We thank Professor A. Collet (Lyon) for helpful discussions. We thank the School of Biochemistry at the University of Birmingham (UK) for providing access to the 500 MHz NMR spectrometer.

Received: November 20, 1996 [F525]

[1] a) J. S. Lindsey, *New. J. Chem.* **1991**, *15*, 153–180; b) G. M. Whitesides, J. P. Mathias, C. T. Seto, *Science* **1991**, *254*, 1312–1319; c) G. M. Whitesides, E. R. Simanek, J. P. Mathias, C. T. Seto, D. N. Chin, M. Mammen, D. M. Gordon, *Acc. Chem. Res.* **1995**, *28*, 37–44; d) D. S. Lawrence, T. Jiang, M. Levett, *J. Am. Chem. Soc.* **1995**, *95*, 2229–2260; e) D. Philp, J. F. Stoddart, *Synlett* **1991**, 445–458; f) D. Philp, J. F. Stoddart, *Angew. Chem. Int. Ed. Engl.* **1996**, *35*, 1154–1196.

[2] a) G. Schill, *Catenanes, Rotaxanes, and Knots*, Academic Press: New York, **1971**; b) D. B. Amabilino, J. F. Stoddart, *Chem. Rev.* **1995**, *95*, 2725–2828.

[3] a) E. Wasserman, *J. Am. Chem. Soc.* **1960**, *82*, 4433–4434; b) G. Agam, D. Graiver, A. Zilkha, *J. Am. Chem. Soc.* **1976**, *98*, 5206–5216; c) I. T. Harrison, *J. Chem. Soc. Chem. Commun.* **1972**, 231–232; d) I. T. Harrison, *ibid.* **1977**, 384–385.

[4] a) R. J. Wolovsky, *J. Am. Chem. Soc.* **1970**, *92*, 2132–2133; b) D. A. Ben-Efraim, C. Batich, E. Wasserman, *ibid.* **1970**, *92*, 2133–2135; c) D. M. Walba, R. M. Richards, R. C. Haltiwanger, *ibid.* **1982**, *104*, 3219–3221.

[5] a) G. Schill, A. Lüttringhaus, *Angew. Chem. Int. Ed. Engl.* **1964**, *3*, 546–547; b) G. Schill, C. Zürcher, *ibid.* **1969**, 988; c) E. Logeman, K. Rissler, G. Schill, H. Fritz, *Ber. Dtsch. Chem. Ges.* **1981**, *114*, 2245–2260.

[6] a) D. H. Busch, N. A. Stepenson, *Coord. Chem. Rev.* **1990**, *100*, 119–156; b) D. H. Busch, *J. Incl. Phenom.* **1992**, *12*, 389–395; c) S. Anderson, H. L. Anderson, J. K. M. Sanders, *Acc. Chem. Res.* **1993**, *26*, 389–395; d) R. Hoss, F. Vögtle, *Angew. Chem. Int. Ed. Engl.* **1994**, *33*, 375–384.

[7] a) C. O. Dietrich-Buchecker, J.-P. Sauvage, J. P. Kintzinger, *Tetrahedron Lett.* **1983**, *24*, 5095–5098; b) C. O. Dietrich-Buchecker, J.-P. Sauvage, *Chem. Rev.* **1987**, *87*, 795–810; c) J.-C. Chambron, C. O. Dietrich-Buchecker, V. Heitz, J.-F. Nierengarten, J.-P. Sauvage, *Transition Metals in Supramolecular Chemistry* (Eds.: L. Fabbrizzi, A. Poggi), Kluwer Academic Publishers: Boston **1994**, p. 371; d) G. J. M. Gruter, F. J. J. Dekanter, P. R. Markies, T. Nomoto, O. S. Akkerman, F. Bickelhaupt, *J. Am. Chem. Soc.* **1993**, *115*, 12179–12180; e) M. Fujita, F. Ibukuro, H. Hagihara, K. Ogura, *Nature (London)* **1994**, *367*, 720–723; f) M. Fujita, F. Ibukuro, K. Yamaguchi, K. Ogura, *J. Am. Chem. Soc.* **1995**, *117*, 4175–4176; g) M. Fujita, F. Ibukuro, H. Seki, O. Kamo, M. Imanari, K. Ogura, *J. Am. Chem. Soc.* **1996**, *118*, 899–900; h) M. Fujita, K. Ogura, *Bull. Chem. Soc. Jpn.* **1996**, *69*, 1471–1482; i) M. Fujita, K. Ogura, *Coord. Chem. Rev.* **1996**, *148*, 249–264; j) C. Piguet, G. Bernardinelli, A. F. Williams, B. Bocquet, *Angew. Chem. Int. Ed. Engl.* **1995**, *34*, 582–584; k) P. R. Markies, T. Nomoto, O. S. Akkerman, F. Bickelhaupt, *J. Am. Chem. Soc.* **1988**, *110*, 4845–4846; l) A. M. Albrecht-Gary, C. O. Dietrich-Buchecker, J. Guilhem, M. Meyer, C. Pascard, J.-P. Sauvage, *Recl. Trav. Chim. Pays-Bas* **1993**, *112*, 427–428; m) J.-C. Chambron, C. O. Dietrich-Buchecker, J.-F. Nierengarten, J.-P. Sauvage, N. Solladie, A.-M. Albrecht-Gary, M. Meyer, *New. J. Chem.* **1995**, *19*, 409–426; n) J. F. Nierengarten, C. O. Dietrich-Buchecker, J. P. Sauvage, *ibid.* **1996**, *20*, 685–693; o) J. L. Weidmann, J. M. Kern, J. P. Sauvage, Y. Geerts, D. Muscat, L. Mullen, *Chem. Commun.* **1996**, 1243–1244; p) D. B. Amabilino, C. O. Dietrich-Buchecker, A. Livoreil, L. Pérez-García, J. P. Sauvage, J. F. Stoddart, *J. Am. Chem. Soc.* **1996**, *118*, 3905–3913; q) D. B. Amabilino, J. P. Sauvage, *Chem. Commun.* **1996**, 2441–2442; r) D. J. Cardenas, A. Livoreil, J. P. Sauvage, *J. Am. Chem. Soc.* **1996**, *118*, 11980–11981.

[8] a) J.-P. Sauvage, J. Weiss, *J. Am. Chem. Soc.* **1985**, *107*, 6108–6110; b) J. Guilhem, C. Pascard, J.-P. Sauvage, J. Weiss, *ibid.* **1988**, *110*, 8711–8713; c) C. O. Dietrich-Buchecker, A.-K. Khémiss, J.-P. Sauvage, *J. Chem. Soc. Chem. Commun.* **1986**, 1376–1378; d) C. O. Dietrich-Buchecker, J. Guilhem, A.-K. Khémiss, J.-P. Kintzinger, C. Pascard, J.-P. Sauvage, *Angew. Chem. Int. Ed. Engl.* **1987**, *26*, 661–663; e) C. O. Dietrich-Buchecker, C. Hemmert, A.-K. Khémiss, J.-P. Sauvage, *J. Am. Chem. Soc.* **1990**, *112*, 8002–8008; f) F. Bitsch, C. O. Dietrich-Buchecker, C. Hemmert, A.-K. Khémiss, J.-P. Sauvage, A. V. Dorsselaer, *J. Am. Chem. Soc.* **1991**, *113*, 4023–4025; g) N. Armaroli, V. Balzani, F. Barigelletti, L. De Cola, J.-P. Sauvage, C. Hemmert, *J. Am. Chem. Soc.* **1991**, *113*, 4033–4035; h) N. Armaroli, V. Balzani, L. De Cola, C. Hemmert, J.-P. Sauvage, *New. J. Chem.* **1994**, *18*, 775–782; i) F. Bitsch, G. Hegy, C. O. Dietrich-Buchecker, E. Leize, J.-P. Sauvage, A. Van Dorsselaer, *ibid.* **1994**, *18*, 801–807; j) N. Armaroli, V. Balzani, F. Barigelletti, L. De Cola, L. Flamigni, J.-P. Sauvage, C. Hemmert, *J. Am. Chem. Soc.* **1994**, *116*, 5211–5217; k) J.-C. Chambron, V. Heitz, J.-P. Sauvage, *Bull. Soc. Chim. Fr.* **1995**, *32*, 340–347; l) J. M. Kern, J. P. Sauvage, J. L. Weidmann, *Tetrahedron* **1996**, *8*, 10921–10934.

[9] a) C. A. Hunter, *J. Am. Chem. Soc.* **1992**, *114*, 5303–5311; b) H. A. Adams, F. J. Carver, C. A. Hunter, *J. Chem. Soc. Chem. Commun* **1995**, 809–810; c) S. Ottens-Hildebrandt, S. Meier, W. Schmidt, F. Vögtle, *Angew. Chem. Int. Ed. Engl.* **1994**, *33*, 1767–1769; d) F. Vögtle, T. Dunnwald, T. Schmidt, *Acc. Chem. Res.* **1996**, *29*, 451–460; e) F. Vögtle, R. Jager, M. Handel, S. Ottens-Hildebrandt, *Pure Appl. Chem.* **1996**, *68*, 225–232; f) A. G. Johnston, D. A. Leigh, R. J. Pritchard, M. D. Deegan, *Angew. Chem. Int. Ed. Engl.* **1995**, *34*, 1209–1212; f) A. G. Johnston, D. A. Leigh, L. Nezhat, J. P. Smart, M. D. Deegan,

ibid. **1995**, *34*, 1212–1216; g) A. G. Johnston, D. A. Leigh, A. Murphy, J. P. Smart, M. D. Deegan, *J. Am. Chem. Soc.* **1996**, *118*, 10662–10663.

[10] a) P. R. Ashton, T. T. Goodnow, A. E. Kaifer, M. V. Reddington, A. M. Z. Slawin, N. Spencer, J. F. Stoddart, C. Vicent, D. J. Williams, *Angew. Chem. Int. Ed. Engl.* **1989**, *28*, 1396–1399; b) P. L. Anelli, P. R. Ashton, R. Ballardini, V. Balzani, M. Delgado, M. T. Gandolfi, T. T. Goodnow, A. E. Kaifer, D. Philp, M. Pietraszkiewicz, L. Prodi, M. V. Reddington, A. M. Z. Slawin, N. Spencer, J. F. Stoddart, C. Vicent, D. J. Williams, *J. Am. Chem. Soc.* **1992**, *114*, 193–218; c) P. R. Ashton, R. Ballardini, V. Balzani, A. Credi, M. T. Gandolfi, S. Menzer, L. Pérez-Garcia, L. Prodi, J. F. Stoddart, M. Venturi, A. J. P. White, D. J. Williams, *ibid.* **1995**, *117*, 11171–11197.

[11] a) P. R. Ashton, C. L. Brown, E. J. T. Chrystal, T. T. Goodnow, A. E. Kaifer, K. P. Parry, A. M. Z. Slawin, N. Spencer, J. F. Stoddart, D. J. Williams, *Angew. Chem. Int. Ed. Engl.* **1991**, *30*, 1039–1041; b) D. B. Amabilino, P. R. Ashton, A. S. Reder, N. Spencer, J. F. Stoddart, *ibid.* **1994**, *33*, 433–437; c) D. B. Amabilino, P. R. Ashton, A. S. Reder, N. Spencer, J. F. Stoddart, *ibid.* **1994**, *33*, 1286–1290; d) D. B. Amabilino, P. R. Ashton, C. L. Brown, E. Córdova, L. A. Godínez, T. T. Goodnow, A. E. Kaifer, S. P. Newton, M. Pietraszkiewicz, D. Philp, F. M. Raymo, A. S. Reder, M. T. Rutland, A. M. Z. Slawin, N. Spencer, J. F. Stoddart, D. J. Williams, *J. Am. Chem. Soc.* **1995**, *117*, 1271–1293.

[12] M. Asakawa, P. R. Ashton, S. Menzer, F. M. Raymo, J. F. Stoddart, A. J. P. White, D. J. Williams, *Chem. Eur. J.* **1996**, *2*, 877–893.

[13] a) P. R Ashton, J. Huff, S. Menzer, I. W. Parsons, J. A. Preece, J. F. Stoddart, M. S. Tolley, A. J. P. White, D. J. Williams, *Chem. Eur. J.* **1996**, *2*, 31–44; b) M. Asakawa, P. R. Ashton, S. E. Boyd, C. L. Brown, R. E. Gillard, O. Kocian, F. M. Raymo, J. F. Stoddart, M. S. Tolley, A. J. P. White, D. J. Williams, *J. Org. Chem.* **1997**, *62*, 26–37; D. B. Amabilino, P. R. Ashton, S. E. Boyd, J. Y. Lee, S. Menzer, J. F. Stoddart, D. J. Williams, *Angew. Chem. Int. Ed. Engl.* submitted.

[14] a) D. Armspach, P. R. Ashton, C. P. Moore, N. Spencer, J. F. Stoddart, T. J. Wear, D. J. Williams, *Angew. Chem. Int. Ed. Engl.* **1993**, *32*, 854–858; b) D. Armspach, P. R. Ashton, R. Ballardini, V. Balzani, A. Godi, C. P. Moore, L. Prodi, N. Spencer, J. F. Stoddart, M. S. Tolley, T. J. Wear, D. J. Williams, *Chem. Eur. J.* **1995**, *1*, 33–55.

[15] a) R. S. Mulliken, *J. Am. Chem. Soc* **1952**, *74*, 811–824; M. J. S. Dewar, J. *Am. Chem. Soc.* **1961**, *83*, 4560–4563; b) R. S. Mulliken, W. B. Parson, *Annu. Rev. Phys. Chem.* **1962**, *8*, 107–126; R. Foster, *Organic Charge-Transfer Complexes*, Academic Press: New York, **1969**; c) R. Foster, *J. Phys. Chem.* **1980**, *84*, 2135–2141; d) C. A. Hunter, J. K. M. Hunter, *J. Am. Chem. Soc.* **1990**, *112*, 5525–5534; e) C. A. Hunter, *Chem. Soc. Rev.* **1994**, 101–109; C. A. Hunter, *J. Mol. Biol.* **1993**, *230*, 1025–1054.

[16] a) R. Taylor, O. Kennard, *J. Am. Chem. Soc.* **1982**, *104*, 5063; b) G. R. Desiraju, *Acc. Chem. Res.* **1991**, *24*, 290–296; c) V. R. Pedireddi, G. R. Desiraju, *J. Chem. Soc. Chem. Commun.* **1992**, 988–990; d) T. Steiner, *ibid.* **1994**, 2341–2342.

[17] a) R. O. Gould, A. M. Gray, P. Taylor and D. Walkinshaw, *J. Am. Chem. Soc.* **1985**, *107*, 5921–5927; b) S. K. Burley and G. A. Petsko, *ibid.* **1986**, *108*, 7995–8001; c) M. Nishio and M. Hirota, *Tetrahedron* **1989**, *45*, 7201–7245; d) M. Nishio, Y. Umezawa, M. Hirota, Y. Takeuchi, *ibid.* **1995**, *51*, 8665–8701.

[18] DNMR 5 (QCPE 569) is an iterative nuclear magnetic resonance program for unsaturated exchange-broadened bandshapes by D. S. Stepenson and G. Binsch, Institute of Organic Chemistry, University of Munich (Germany). (QCPE 365) converted and modified by C. B. Lemaster, C. L. Lemaster, N. S. True, Department of Chemistry, University of California, Davis, California 95616 (USA).

[19] P. R. Ashton, C. G. Claessens, W. Hayes, S. Menzer, J. F. Stoddart, A. J. P. White, D. J. Williams. *Angew. Chem. Int. Ed. Engl.* **1995**, *34*, 1862–1865.

[20] a) Compound **5a** was prepared according to the procedure described in: P. R. Ashton, E. J. T. Chrystal, J. P. Mathias, K. P. Pary, A. M. Z. Slawin, N. Spencer, J. F. Stoddart, D. J. Williams, *Tetrahdron Lett.* **1987**, *28*, 6367–6370; b) Compound **5c** was prepared according to the procedure described in: R. E. Gillard, J. F. Stoddart, A. J. P. White, B. J. Williams, D. J. Williams, *J. Org. Chem.* **1996**, *61*, 4504–4505.

[21] Values for k_c were obtained (I. O. Sutherland, *Annu. Rep. NMR Spectrosc.* **1971**, *4*, 71–235) using the approximate expression $\pi(\Delta\nu)/(2)^{1/2}$, and the Eyring equation was then used to calculate $\Delta G_c^{\ddagger}$ at the coalescence temperature T_c.

[22] Note that $\Delta\nu = 492$ Hz at 263 K ($T_c = 291$ K, 400 MHz) for the hydroquinone ring protons of the crown ether moiety in **6b**·4PF$_6$.

[23] Note that $\Delta\nu = 94$ Hz at 180 K ($T_c = 198$ K, 400 MHz) for the β-CH bipyridinium protons in **6b**·4PF$_6$.

[24] Note that $\Delta\nu = 50$ Hz at 188 K ($T_c = 200$ K, 400 MHz) for the β-CH bipyridinium protons and $\Delta\nu = 48$ Hz at 188 K ($T_c = 197$ K, 400 MHz) for the hydoquinone ring protons of the tetracationic cyclophane in **6c**·4PF$_6$.

[25] D. D. Perrin, W. L. Armarego, *Purification of Laboratory Chemicals*, 3rd ed., Pergamon Press: New York, **1988**.

[26] SHELXTL PC version 5.03, Siemens Analytical X-Ray Instruments, Inc., Madison, WI, **1994**.

0947-6539/97/0305-0798 $ 17.50+.50/0